ICE, CLOUD, AND LAND ELEVATION SATELLITE-2 (ICESat-2)
ATL12 Ocean Surface Height Release 007
Application Notes and Known Issues

Jamie Morison, PSC
Suzanne Dickinson, PSC
David Hancock, GSFC
Leeanne Roberts, GSFC
John Robbins, GSFC

10/27/2024

Introduction

This document contains notes for the use of the ICESat-2 ATL12 Ocean Surface Height product. It includes issues that are known to the developers, which may be fixed in future releases of this product. Feedback from the community will be added to future revisions of this document.

Table of Contents

Notes: The ATL12 Ocean Surface Height Product Philosophy and Brief Description

The Ice, Cloud, and Land Elevation Satellite-2 (ICESat-2) provides satellite ocean altimetry unlike any other. ICESat-2 has been developed primarily to measure the height of the Earth's ice and land at high spatial resolution. To achieve this resolution it carries the Advanced Topographic Laser Altimeter System (ATLAS), a photon-counting, multi-beam lidar pulsing at 10 kHz. At the speed of the spacecraft, each beam of ATLAS illuminates 15 m patch of the surface every 0.7 m of along-track distance. Given the low reflectance of the ocean surface, of all the photons detected by ATLAS, on the order of one photon per pulse returns from the ocean surface. ATLAS determines the apparent height of the reflecting surface for each one of these photons along with the apparent height of a lower density of noise photons. Averaged over along-track distance these heights form a histogram of heights reminiscent of the waveforms of other radar (e.g., CryoSat-2) and analog lidar (e.g., ICESat-1) satellite altimeters, and thus we are tempted to think in terms of "retracking" to decide what part of this "waveform" represents the average ocean surface over a "foot print" corresponding to the averaging distance.

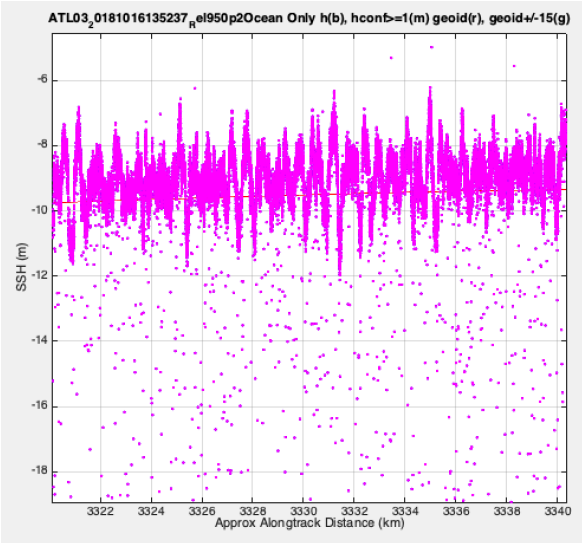

Figure 1. ATL03 photon heights (magenta) from Oct. 16, 2018 over the Pacific Ocean and the EGM2008 geoid (red line). Waves in the dense photon cloud are apparent as well as subsurface and atmospheric noise photons.

We have adopted a different philosophy in processing the ICESat-2. We do not think in terms of "footprint" and "retracking" in the usual way but treat every photon height documented in the ATL03 data product input to ATL12 as an individual point measurement of surface height averaging less than a meter apart, but with a x-y location uncertainty on the order of 10 m. Figure 1 shows ATL03 photon heights collected over ~20-km of ocean surface. The dense cloud of heights representing surface-reflected photons clearly stands out from the lower density of noise photons above and below and reveals surface waves with about 2.5 m significant wave height (SWH) and an apparent 470-m wavelength. In processing, we first distinguish by a histogram trimming method, which of these heights over an adaptively chosen ocean segment length (typically 7-km) are from true surface reflected photons versus noise photons. The resultant "received height histogram" is deconvolved with an instrument impulse response (IIR) histogram representing the height uncertainty associated with the lidar transmit pulse width and other instrumental factors. This produces a surface height histogram that, with its first four moments, is the primary ATL12 products. In addition we analyze the spatial series of surface photons heights to characterize surface waves and calculate the correlation of photon return rate and surface height that constitutes the EM sea state bias (SSB) in the mean sea surface height (SSH).

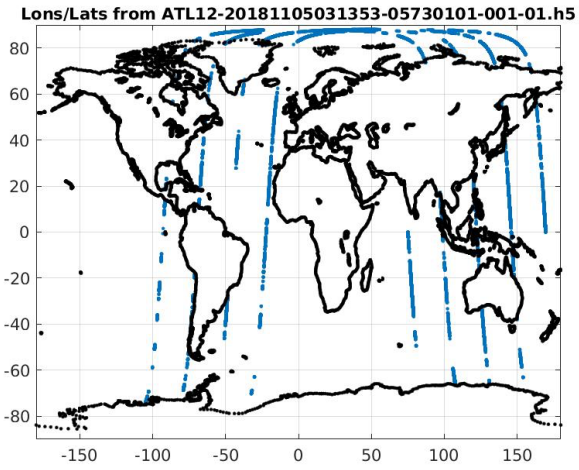

Figure 2. Example of ocean segment locations (latitude, longitude) for a single ATL12 granule, comprising four orbits.

Thus, the ATL12 Ocean product includes histograms and statistics of sea surface height over variable length along-track ocean segments. The processing has been designed around open ocean conditions and includes a sea state bias calculation. However, the processing is run over the world ocean including ice-covered regions covered by ATL07 and ATL10. In these regions, the statistical products will be valid statistics for the mixed ice-covered and ice-free surface, but mean heights will include the average freeboard of sea ice.

ATL 12 photon heights are derived from the ATL03 ocean photon height data with signal confidence level 1 or higher and within 15 m of the EGM2008 geoid. Signal confidence 2, 3, and 4 correspond to low, medium, and high confidence the photon is surface reflected and confidence level 1 fills a ±15-m buffer about the high confidence level photon heights. This constraint, along with the geoid band criteria, have been found to edit out heights in erroneous downlink bands associated with high background noise rates.

From this population, we first accumulate photon heights likely to fall within the distribution of ocean surface heights until 8,000 candidate photons or 7 km of along-track distance is traversed. All the photons over the resulting ocean segment are then subjected to two iterations selecting photon heights in the histogram at levels above the background rate. After the first iteration, a linear trend and average height is removed from the heights prior to the second iteration. The trend and average height are retained for output as part of the ocean segment statistics. From there the height data follows two paths

The histogram path considers the histogram of the received ocean segment heights and deconvolves the histogram of the instrument impulse response to produce the surface height distribution. This is then fit with a 2 Gaussian mixture to produce the first four moments of the surface height distribution. The derived height surface histogram and the four moments comprise the main the ATL12 data products

The space series track maintains the surface heights as an along-track series and by correlating the photon return rate with surface height at 10-m along-track scale, estimates significant wave height and the EM sea state bias (SSB) ATL12 data products. In future releases, analyses on this track will include more wave properties and estimates of statistical degrees of freedom for the accumulation gridded statistics in the ATL17 gridded data product.

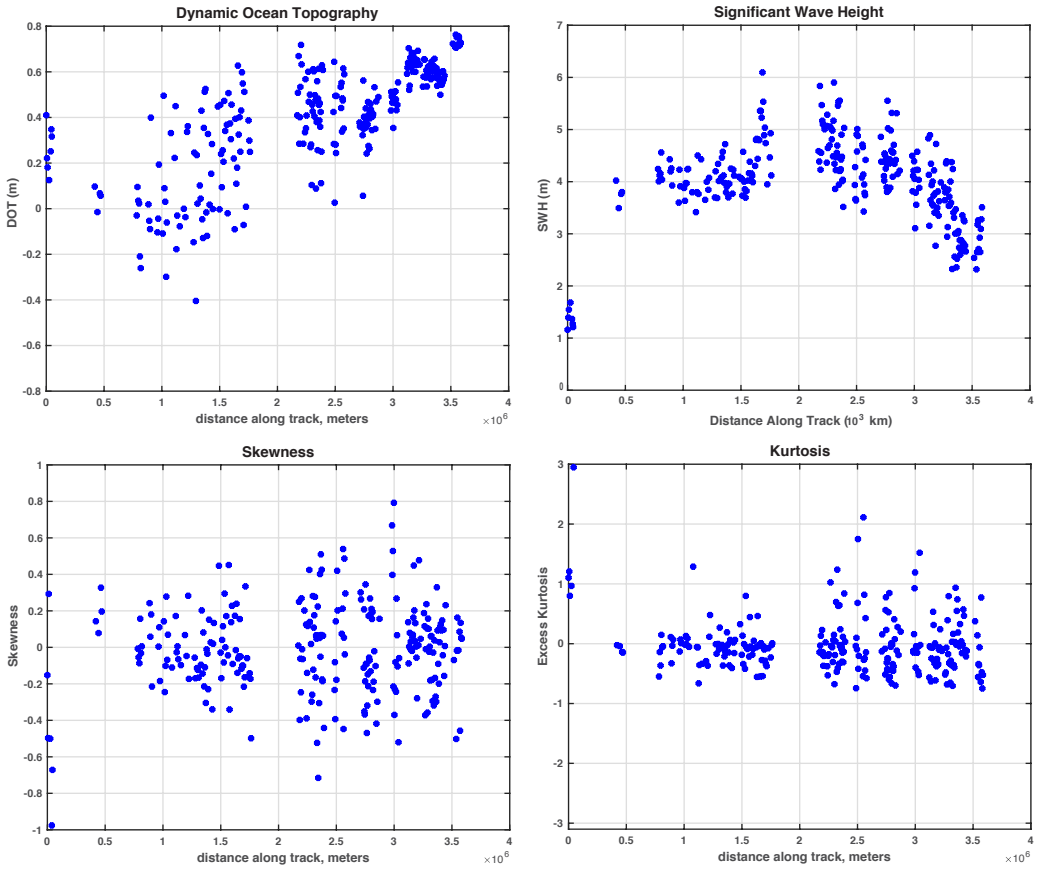

Figure 3. ATL12 ocean segment statistics. Upper left: mean SSH, upper right: significant wave height = 4 x standard deviation, lower left: skewness of sea surface height, lower right: kurtosis of sea surface height. Yellow DOTS are ATL12 ASAS 5.1 and blue dots are from our developmental Matlab code applied to ATL03, which generally does not segment the data exactly the same as ATL12. ASAS 5.1 and Matlab agreement is better where segments are more closely matched.

Each ATL12 data file covers the world ocean over four consecutive ICESat-2 orbits (Fig. 2). ATL12 file names such as ATL12_20181105031353_05730101_001_01.h5 include the date/time sequence (yyyymmddhhmmss=20181105031353) of the start of the first orbit, the reference ground track (_####=_0573), the cycle (##=01), the region (##=01), and the release (###=001).

The processed data are for areas designated as ocean according to the ICESat-2 ocean surface mask. The ocean mask overlaps with the other surface types in buffer zones up to 20-km wide. Consequently, early releases of ATL12 data included bands that were in fact not open ocean but which were close enough to sea level to fall within ±15 m of the geoid, close enough to be accepted by ATL12's processing. Examples were the marginal sea ice zones under the sea ice surface type and low-lying islands under the land surface type. Release 3 processing includes a bathymetry test to ensure the ATL12 processing covers only ocean waters. For each 20-m geo-segment, the corresponding depth from the General Bathymetric Chart of the Oceans (GEBCO, https://www.gebco.net) database is used to determine water depth, and ATL12 processing is done for depths greater than 10-m. As an added benefit, the average GEBCO depth over each ocean segment is output as another Release 3ATL12 data product.

Except in special cases or when overlapping one of the other surface types, over the ocean only the three strong beams with ground tracks separated by 3 km are downlinked by ATLAS. The ATL12 software processes each strong beam independently. An example of ocean statistics measure by the middle strong beam over one ATL03 granule in the North Pacific is shown in Figure 3 for all ocean segments in the granule.

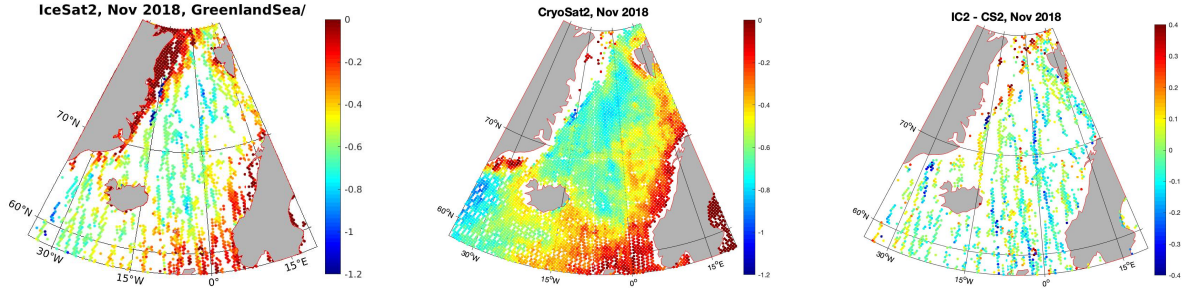

Figure 4. ICESat-2, CryoSat-2 dynamic ocean topography (DOT in meters) comparison for the Greenland Sea in November 2018. Left: ICESat-2 from ATL12 Rel001, bin-averaged in a 25-km grid. In this case ocean and sea ice mask data are included. Center: CryoSat-2 LRM and pLRM from RADS bin-averaged in a 25-km grid. These are open water products. Right: ICESat-2 DOT minus CryoSat-2 DOT bin-averaged in a 25-km grid. Differences are taken only for grid cells with both ICESat-2 and CryoSat-2 data.

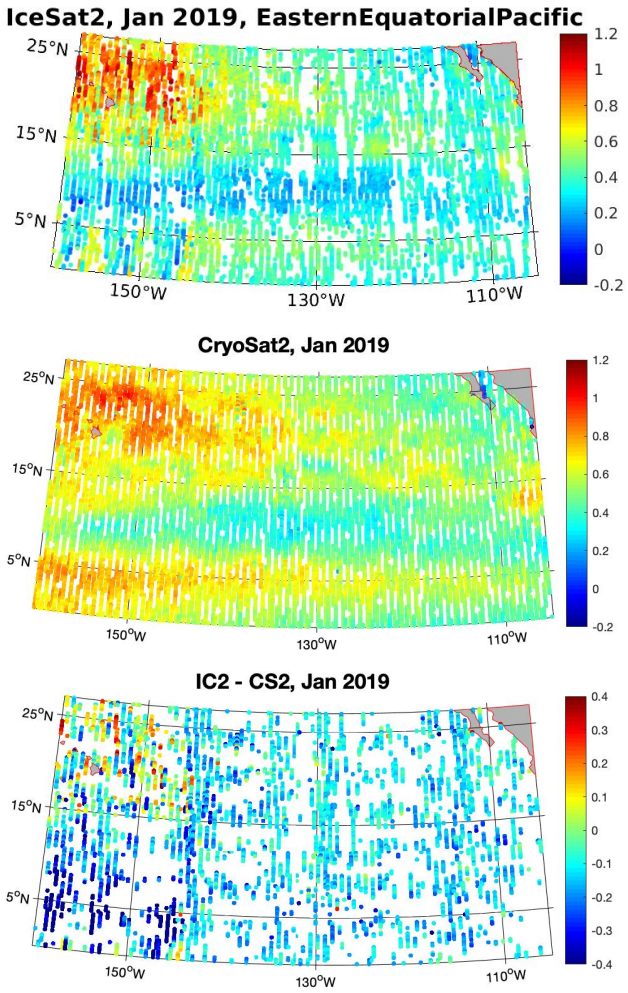

Figure 5. ICESat-2, CryoSat-2 dynamic ocean topography (DOT) comparison for the Eastern Equatorial Pacific in January 2019. Top: ICESat-2 DOT (m) from ATL12 Rel001, bin-averaged in a 25-km grid, Center: CryoSat-2 DOT (m) LRM and pLRM from RADS bin-averaged in a 25-km grid, Bottom: ICESat-2 DOT minus CryoSat-2 DOT (m) bin-averaged in a 25-km grid. Differences are taken only for grid cells with both ICESat-2 and CryoSat-2 data.

Our first efforts at calibration and validation of ICESat-2 SSH show good agreement with CryoSat-2, especially in the Sub-Arctic Seas. Figure 4 shows comparison of ICESat-2 and CryoSat-2 dynamic ocean topography, DOT=SSH-Geoid (EGM08) for the month of November 2018 bin-averaged in a 25-km grid. ICESat-2 did not get as many surface measurements as CryoSat-2, almost surely due cloud cover over the November Greenland Sea. However, the same DOT patterns such as DOT set up towards the coasts associated with the East Greenland, Norwegian, and West Spitzbergen currents are almost identically shown in both data sets. The difference between gridded ICESat-2 and CryoSat-2 DOT is on the right of Figure 4. Over all the grid cells with ICESat-2 and CryoSat-2, ICESat-2 DOT is 0.64 cm higher than CryoSat-2 DOT ± 16.6 cm standard deviation. This comparison is remarkable given the early release of ICESat-2.

Figure 5 is similar to Figure 4 except the comparison is done for the Eastern Equatorial Pacific (EEP) for January 2019. In spite of a lower density of ground tracks at low latitude, ICESAt-2 data coverage in the EEP is arguably better than in the Greenland Sea, likely because of clearer sky conditions. The ICESat-2 and CryoSat-2 DOT patterns in the EEP are very similar, showing among other things the trough along 5°N likely associated with North Equatorial Current and North Equatorial Counter Current. The similarity breaks down a little in the western part of the area with ICESat-2 DOT being a little higher than CryoSat-2 DOT in the northwest and lower than CryoSat-2 DOT in the southwest. On average ICESat-2 DOT is 13.1 cm lower than CryoSat-2 DOT ±12.2 cm standard deviation. This is not as good as the Greenland Sea comparison but comparable in magnitude to other ICESat-2 ground truth comparisons for this release.

Issues

The issues below are those that could affect use of ATL12 Rel. 007 presently or could affect changes in the way ATL12 data are used in the future.

Issue 1. Surface Finding, Subsurface Returns, and Histogram Trimming

Distinguishing surface reflected photon heights involves establishing a histogram of all heights in an ocean segment and then searching outward from the center of the histogram to find high and low limits where the histogram level falls below an estimate of the noise level. The photon heights between the high and low limits are considered surface photon heights. To determine the high and low limits, earlier releases compared a smoothed version of the histogram to the median value of the smoothed histogram. Because with the small bin size (1-cm) of the current processing, the median of the smoothed histogram usually reflects the noise tails, and the resulting trimming worked reasonably well. However, it treated the subsurface and above surface tails of the histogram the same.

Because the blue-green laser of ATLAS penetrates water, true subsurface returns have always been a concern, and the higher subsurface density of photons apparent in Figure 1 may be due in part to subsurface scattering in the ocean. However, we see similarly enhanced subsurface densities over, clear deep ocean waters and even over land where penetration and backscatter shouldn't occur. Consequently present thinking expressed in the ATL03 known issues is that the subsurface noise level is due, at least in part, to forward scattering delays in the atmosphere of surface reflected photons.

Whatever their cause, some subsurface photon heights are included in the raw surface height histogram, creating what was an order 1-3 cm bias in average SSH in previous releases. To reduce the sensitivity to subsurface returns, the ASAS code for Release 4 and higher bases surface finding not on a histogram of raw surface height, but on the photon height anomaly about an 11-point moving average of the high confidence photons (confidence level from ATL03 greater than or equal to 3). This moving average does a reasonable job of following large surface waves so that anomalies from it can distinguish subsurface returns versus returns from the troughs of large waves. The Release 4 and higher processing makes a simple estimate of the high and low limits of the anomaly histogram and then uses these to determine separate above-surface and sub-surface noise levels. The ultimate high limit is then chosen where the smoothed anomaly histogram falls below a factor (e.g., 1.5) times the above surface noise and the low limit is chosen where the smoothed histogram falls below the same factor times the subsurface noise. In testing this approach eliminates more subsurface returns, particularly under wave crests, than were excluded in prior releases with surface finding based on the photon height histogram rather than height anomaly histogram.

Issue 2. Uncertainty in Mean SSH

We have found the wave environment, rather than instrumental factors, is probably the biggest contributor to uncertainty in estimates of the mean SSH. This is illustrated by our analysis of multiple ocean segments, of which the data of Figure 1 is one 7-km ocean segment in the southern part of the central North Pacific. These segments show variability in their mean sea surface heights of approximately ± 0.12 m, much greater than we'd expect from instrumental factors. The standard error, σ_L, in the estimates of the mean are given by

$$\sigma_L = \sigma_h \left(N_{df} \right)^{-1/2}$$

where σ_h is the standard deviation of the population and N_{df} is the number of degrees of freedom. If every one of the ~ 8,000 photon heights were independent, even with a SWH = 2.5 m (σ_h = .625 m), the uncertainty in estimates of the mean would be less than 1 cm. The problem is that owing to the presence of long large waves, successive photon heights are far from independent. The fact that the underlying wave signal is periodic makes the estimate of the effective degrees of freedom problematic. As a worst case if we set N_{df} equal to the number of wave periods in the ocean segment, 15 in the case Figure 1, the uncertainty, σ_L, in the estimate of the mean equals 0.16 m, close to what we see over many similar ocean segments. This problem is not instrumental; it is just made apparent by the ability of ICESat-2 to resolve waves.

To lower this uncertainty, we explored using harmonic analysis of surface height over each ocean segment and use of the zero wave-number amplitude to represent SSH (D. Percival, personal communication, 2019) as a way of removing large periodic variations in height as a cause of uncertainty. This approach did not make a significant difference in ocean segment average sea surface heights. The uncertainty is inherent in measuring SSH over a wave-covered surface. However, the harmonic analysis is included in ATL12 Release 4 and above to add a measure of wave spectral properties.

Estimates of effective degrees of freedom and uncertainty in Release 4 and above are based on an autocorrelation analysis of 10-m along-track binned surface heights each ocean segment. These properly account for uncertainties in the ATL12 ocean segment averages of SSH and DOT and will be used in derivation of the ATL19 gridded DOT product.

Issue 3. Erroneous Downlink Bands

In order to conserve bandwidth over the ocean, the Flight Science Receiver Algorithms (FSRA) on board ICESat-2 selects photons in a downlink band currently 50-m in vertical width (See ATL03 Users Guide). This band is centered over where FSRA detects the highest concentrations of photons. Signal confidence equal to 2, 3, 4 correspond to low, medium, and high confidence that the photon is a surface return. Signal confidence equal to 1 is applied to the remaining no confidence photons filling a band ±30-m around the high confidence photons. As long as the background photon count is low at night or in clear conditions this band will be centered on the ocean surface near the geoid. But in daylight with scattered clouds, the downlink band can shift to unrealistic heights or depths for 200-pulse major frames. To reduce this problem, for Release 4 and beyond, ATL03 only keeps downlinked photons within 30 m of DEM, or geoid in the case of the ocean. In any event, to avoid erroneous downlink bands for Release 4 and above, the ATL12 ASAS code selects a band that includes photons with a signal confidence greater than or equal to 1 and falling within ±15-m of the EGM2008 geoid.

Issue 4. Sea Surface Heights Among Beams

Our cal/val comparisons with CryoSat-2 (Figs. 4 and 5) had been performed for the center strong beam only. In developing the ATL19 gridded product processing we experiment with gridding DOT separately for each beam. For an ATL12 derived from an experimental ATLO3 made with the current orbit and pointing determinations as used in ATL03 Release 4 and beyond, we find the biases between all but one of the beams are less than 1 cm.

Issue 5. Bathymetry Test and Surface Type

As mentioned in the notes, releases after Release 3 include a bathymetric test based on GEBCO ocean depth greater than 10-m to insure the ATL12 processing covers only ocean waters. It also

includes ocean segment average depth as an output. The user can gain an appreciation of how much non-open ocean is included in an ocean segment by looking at the *gtxx/ssh_segments/stats/surf_type_prcnt* output variable that gives the percentage of the ocean segment covered by each surface type covered in an ocean segment. (Be advised that the surface type from 1 to 5 denote land, ocean, sea ice, land ice, and inland water as listed in ATL03).

Issue 6. SSB Calculation

We estimate the Sea State Bias (SSB) due to variations in sampling over surface waves. The electromagnetic (EM) sea state bias occurs for example if more photons tend to be returned from wave troughs than from wave crests. This SSB is equivalent to the covariance of photon return rate and sea surface height divided by the average photon return rate. We estimate this with the return rates and heights averaged in 10-m along track bins. The SSB estimates have been smaller than we have expected ~-1.2 % of Significant Wave Height (SWH). Note that the SSB parameter is an estimate of sea state bias and should be subtracted from the heights output by ATL12 Release 4 and above to correct the heights for sea state bias. Also note, typical radar altimeters show an SSB of about – 4% and we have found ICESat to have no SSB below SWH= 2 m, but -18% of SWH above 2 m [*Morison et al.*, 2018]. ICESat-2 appears to be less sensitive to SSB. Also note, our ICESat-2 SSB is an *a priori* prediction based on EM bias. It doesn't include SSB due to retracker design or assumptions about waveform or surface height distribution, but then ICESat-2 processing doesn't involve retracking and assumptions about waveform or surface height distribution. Indeed, the ATL12 measures the surface height distribution and its first four moments.

In a study that is currently underway, several of us are comparing ICESat-2 ATL12 and 19 Release 6 sea surface heights with radar altimeter sea surface heights, and our findings suggest the differences are due to differences between the SSB for radar altimeters versus the EM SSB calculated ICESat-2. Alexa Putnam has compared ICESat-2 ATL12, open ocean SSH with along-track altimetry from Jason-3 and Sentinel-6 Michael Freilich and finds close agreement in heights uncorrected for sea state bias (SSB). However, when the respective SSB corrections are applied, ICESat-2 over the mid latitudes (60°S to 60°N) averages about 8-cm lower than the radar altimeters. The difference is effectively the same, 8.5-cm, when we compare ICESat-2 ATL19 gridded DOT, which includes the ICESat-2 SSB correction, with radar altimeter Aviso CMEMS gridded DOT computed by Patricia Vornberger, John Robbins and David Hancock of the ICESat-2 Project Office. However, the average difference is only 2.8 cm between ATL19 and CMEMS in the northern band (30°N to 60°N) and 4.8 cm in the southern band. The larger overall bias seems to come from the tropical band (30°S to 30°N) where the average bias is 10.4 cm. This is surprising, given the significant wave heights are lowest in the tropical band, and we expect SSB there to be small, although the SWH from radar altimeters at less than 2-m significantly increase in uncertainty as a result of retracker resolution and measurement compression. Our hypothesis, which we want to investigate further under a separate study proposed to the NASA Ocean Surface Topography Science Team, is that the ICESat-2 versus radar altimeter bias is due to the aliasing of natural negative correlations between sea state and DOT into the derivation of the radar altimeter SSB, resulting in a positive radar altimeter SSB correction that is too great. To this point, in a paper we found since we submitted our proposal, *Hausman and Zlotnicki* (2010) indicate the alaising problem does not affect the SSB determinations from DOT and SWH correlations between samples only 10-days apart because of the latency in the response between wind and DOT except the variations due to Equatorial

Kelvin waves and the barotropic response at high latitudes. Appropriate to the latter, *Wearn & Baker* (1980) find the Antarctic Circumpolar Current (ACC) transports are correlated with Southern Ocean wind stress lagged nine days. Further, we find in 5-years of ATL23 gridded DOT (corrected for SSB) and SWH, the seasonal correlations of DOT and SWH are quite negative, -0.7. If even a little of these seasonal correlations leak into the 10-day window it could negatively bias the SSB determination resulting in a positive bias of radar altimeters versus ICESat-2. By comparing ICESat2 and radar altimeters, we seek to resolve this issue and improve the SSB corrections of both.

Issue 7. Quasi-specular returns and first-photon bias

Related to the SSB calculation issue, ATL07 results near the ice edge sometimes show reduced SSH near the ice edge (*Ron Kwok*, personal communication). It has been hypothesized that this is due to quasi-specular returns from the troughs of waves. We have not as yet investigated this hypothesis with our SSB calculation but the CryoSat-2 versus ICESat-2 comparisons of Figure 4 (right) suggest that the problem is not affecting ICESat-2 ATL12 at the Greenland Sea ice edge.

However, we occasionally see regions of photon return rates ten times higher than normal in the open ocean. These regions of quasi-specular returns are usually areas without large wind waves, and we think they are also areas where small ripples effectively broaden the angular dependence of reflectance just enough to give strong returns within a few degrees of nadir incidence. This may result in positive height bias over surfaces producing quasi-specular returns.

Not anticipating such high reflectance from the ocean, we have not implemented a correction, *fpb_corr*, for photon detector saturation in ATL12 releases prior to Release 7, but associated with adapting ATL12 and ATL19/23 in the presence of sea ice, and the consequent use of the 10-m data in quasi-specular "bright leads" for DOT determination in the presence of sea ice, we have implemented first photon bias correction, *fpb_corr*, using the Tony Martino model of ATL03 and ATL07. Release still rejects data with full saturation and averages the saturation flags as by *full_sat_fract_seg* and *near_sat_fract_seg.*

Issue 8. Ice versus Sea Surface Height in Sea Ice Covered Regions

Sea ice regions fall under the Sea Ice Surface mask where sea ice surface height (ATL07), and freeboard and sea surface height anomaly (ATL10) are determined. The sea ice surface mask is defined as that part of the ocean where sea ice concentrations (from passive microwave remote sensing) are greater than 15%. However, sea ice regions also fall under the ocean mask. Consequently, the user will find ATL12 sea surface heights in ice-covered regions, and prior to Release 7, these have been biased above the true sea surface height by the freeboard of the ice. As with Issue 5, the user can gain an appreciation of how much sea ice is included in an ATL12 ocean segment by looking at the *gtxx/ssh_segments/stats/surf_type_prcnt* output variable that gives the percentage of the ocean segment covered by each surface type in an ocean segment.

However, we would like our sea surface height and dynamic ocean topography determinations in ATL12 and ATL19/23 to be valid across the whole North Polar and South Polar areas from open water to ice-covered regions, i.e., even in ice concentrations greater than 15%, without being biased by sea ice freeboard. To do this in Release 7 of ATL12 and ATL19/23 we use information from ATL07 to determine DOT as measured in the same ice-free "bright leads" used to determine sea surface height in ATL07.

This requires measurements of height at a fine enough horizontal scale to resolve leads in sea ice. We have these in the ATL12 10-m averages for leads greater than 10-m wide. In Release 7, we align ATL12 and simultaneous ATL07 along-track records and determine which ATL12 10-m bins are judged to be open water bins according to the ATL07 *height _segment_ssh_flag* identifying ATL07 height segments as "bright" open-water surfaces that have a quai-specular photon return rate. ATL10 uses an additional ATL07 parameter to characterize the quality of fit of photon heights to the idealized ATLO7 photon height distribution, *height_segment_fit_quality_flag,* and requires *fit_quality_flag* to be 1, 2, 3, or 4 for use of the segment height for sea surface height. For ATL12 we use the same criteria, ATL07 *ssh_flag*=1 and *fit_quality_flag* = 1, 2, 3, or 4 to consider the ATL07 segment height suitable for SSH or DOT determination. So, we flag the ATL12 10-m bins so qualified by ATL07 as valid "bright" open water with flag consisting of the corresponding ATL07 sea ice segment height converted to DOT, *xbin_atl07_dot*, relative to the EGM2008 geoid. Also, where ATL07 uses the dynamic inverted barometer correction, we remove it and apply the dynamic atmospheric correction used in ATL12. (Note: we believe the DAC is a more appropriate correction even in ice covered waters. If in future releases of ATL07, the DAC is used, this conversion won't be necessary.) With these adjustments we compute the ATL07 DOT for each 10-m bin identified as being in an ATL07 "bright" lead, *xbin_atl07_dot*.

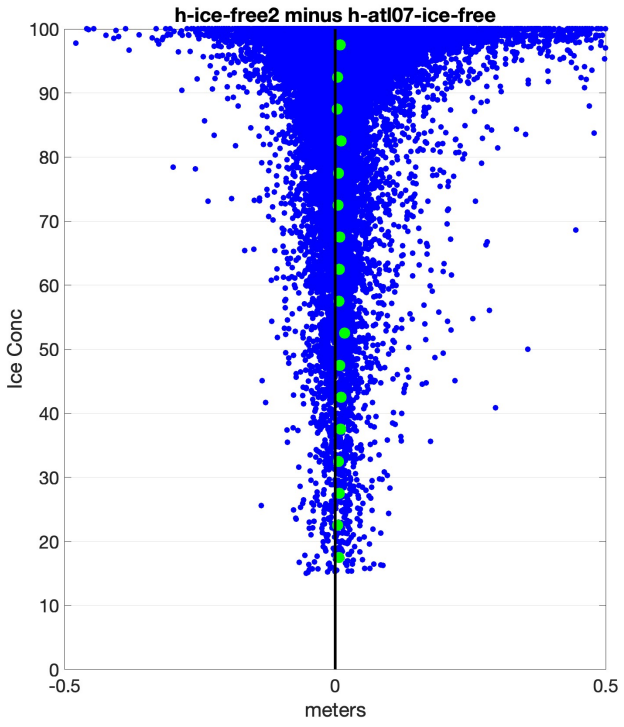

Ice Conc	Mean Diff	STDev Diff
2.5		
7.5		
12.5		
17.5	0.0069	0.0344
22.5	0.0041	0.0340
27.5	0.0076	0.0377
32.5	0.0063	0.0269
37.5	0.0103	0.0373
42.5	0.0108	0.0436
47.5	0.0084	0.0412
52.5	0.0170	0.0824
57.5	0.0067	0.0414
62.5	0.0075	0.0429
67.5	0.0086	0.0523
72.5	0.0052	0.0439
77.5	0.0064	0.0448
82.5	0.0110	0.1375
87.5	0.0038	0.0583
92.5	0.0045	0.1106
97.5	0.0090	0.0712

Figure 6. Plot (left) and table (right) of *h_ice_free* minus *h_atl07_ice_free* versus ice concentration. Overall average *h_ice_free* - *h_atl07_ice_free* =0.0086 ±0.075. For ice concentration < 77.5%, biases are ~ 1 cm ± 4 cm

Note: we limit candidate bins for sea surface height determination to those 10-m bins for which the photon return rate, *xrbin*, is between 4 and 25 photons per meter (strong beams) or 1 to

7 photons per meter (weak beams) corresponding to quasi-specular but not fully saturated returns. This is a wider range than the criteria for ATL07 segments to have *ssh_flag*=1, indicating bright leads.

When we account for first photon bias (see Issue 7 above), ATL12 heights in the 10-m bins so flagged can also be considered ice-free sea surface heights. The average over the ocean segment (termed *h_ice_free*) of these qualified ATL12 sea surface DOT heights and the average over the ocean segment (termed *h_ATL07_ice_free*) of the corresponding ATL07 *xbin_atl07_dot* are added to the ATL12 Release 7 product to provide ATL12 and ATL07 renditions of ATL12 ocean segment ice-covered DOT. These two measures can be compared as an indication of how accurate it is to assume surface finding over open water produces the same result in ATL12 and ATL07.

We also identify all the ATL07 sea ice segments with *ssh_flag*= 1 (bright leads) in an ATL12 ocean segment and compute *h_atl07dot_inatl12oc*, the average DOT from all these ATL07 *ssh_flag* =1 qualified sea ice segments regardless of whether they have a corresponding ATL12 10-m bin. This is important where there are only leads smaller than 10-m in the span of an ATL12 ocean segment.

Testing of the AL12 DOT determination indicates *h_ice_free* and *h_atl07_ice_free* agree at the 1-cm level for ice concentrations less than 77.5% (Fig. 6)

Issue 9. Spikes in ATL12 DOT and SSH Values

Dynamic ocean topography (DOT), in addition to being the determinant of surface geostrophic circulation, provides an excellent check on the final ATL12 sea surface height product. DOT is equal to sea surface height corrected for sea state bias minus the geoid (*gtxx/SSH_segment/heights/h - gtxx/SSH_segment/heights/bin_ssbias - gtxx/SSH_segment/stats/geoid_seg*)*. Reasonable values are within a meter or two of zero, and in the current release this is mainly true world-wide (Fig. 7) but there are unrealistic spikes in DOT (Fig. 8). These seem to come in two varieties.

a) We find numerous large DOT spikes (order several meters) near the ice edges (Fig. 8 upper in blue). These are likely rough ice signatures. They are especially bad in the Antarctic seasonal sea ice zone and we find the larger spikes are due to returns off ice shelves and icebergs, which are included in the ocean mask.

b) At mid and tropical latitudes (Figure 8 upper in red), there are spikes that we have learned are associated with maneuvering the ICESats-2 spacecraft in Drag Make Up (DMU) operations. There are about 5-6 DMUs per month lasting about an hour each, and when they occur, they may affect 10-15% of the ocean segments in the ATL12 file so afflicted.

Related DMUs, ICESat-2 performs conical “Ocean Scans” to check the pointing calibration. These are commonly over the western Pacific. During the scans, the incidence angle is increased to 5° and we find the heights develop substantial inter-beam biases and should not be used for ocean height measurement and should not be trusted.

Consequently, in Release 5 and above we use the *podppd_flag* to edit these data. The flag has seven possible values: normal operations vales: 0=NOMINAL; 1=POD_DEGRADE; 2=PPD_DEGRADE; 3=PODPPD_DEGRADE; plus possible calibration maneuver related "CAL" values: 4=CAL_NOMINAL; 5=CAL_POD_DEGRADE; 6=CAL_PPD_DEGRADE; 7=CAL_PODPPD_DEGRADE. For ATL12, we only use data when the POP/PPD flag indicates nominal normal operations or nominal CAL maneuvers, ***podppd_flag*** equal to 0 or 4. For each ocean segment processed, we report the higher of these two ***podppd_flag*** values, 0 or 4, of data used in the ocean segment.

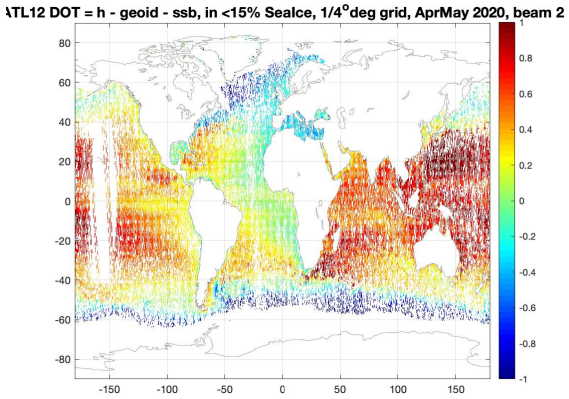

Figure 7. ATL12_20200401021904_00850701_003_01.h5 to ATL12_20200513123852_07330701_003_01.h5 DOT averaged in ¼° bins for sea ice concentration <15%.

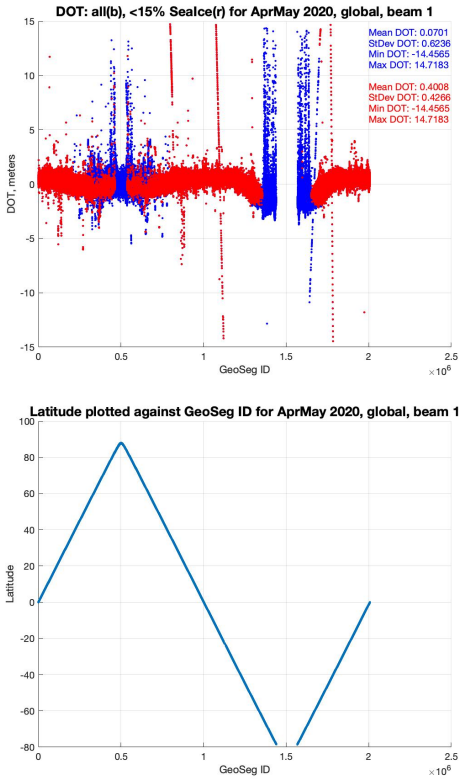

Figure 8. DOT versus ocean segment ID (upper) and ocean segment latitude versus ocean segment ID (lower).

c) In separate work, looking at ATL12 DOT around Greenland, we also found unrealistic spikes in sea surface height that may or may not be due to ice or POP/PPD issues. To avoid these getting into the ocean gridded product, ATL19, we will pre-filter ATL12 data with a 2-pass, 3-sigma filter on DOT. This is may be a good overarching approach for other ATL12 users as well.

Issue 10. Surface Type Percent Scaling

The ocean segment average surface type percentage for ocean, *surf_type_prcnt* category 2, should equal 100% because an ocean depth criterion, depth > 10 m, is used to decide where to compute ocean segment averages. Because of overlap regions between the various surface masks, there can also be significant percentages of other surface types less than or equal to 100%. This scaling will always yield a corrected value for ocean ***surf_type_prcnt*** of 100%. Non-ocean surface types will commonly have values of zero or 100%, with occasional values falling in between, for those segments located in a surface type mask transition zone. Consequently, the sum of percentages in the five different categories will be greater than or equal to 100%.

Issue 10. Unknown Issues

At present, we have only seen limited amounts Release 7 ATL03 samples scattered through 2019. Consequently, there may be a number of issues, particularly with respect to the DOT in ice-covered waters, that remain to be discovered when Release 7 ATL03 and ATL07 (for ice-covered waters) come out.

References:

Hausman, J., and V. Zlotnicki (2010), Sea State Bias in Radar Altimetry Revisited, *Marine Geodesy*, *33*(sup1), 336-347, doi:10.1080/01490419.2010.487804.

Morison J., R. Kwok, S. Dickinson, D. Morison, C. Peralta-Ferriz, and R. Andersen (2018), Sea State Bias of ICESat in the Subarctic Seas, *IEEE Geoscience and Remote Sensing Letters*, 15 (8), 1144 - 1148, DOI: 10.1109/LGRS.2018.2834362

Wearn, R. B., & Baker, D. J. (1980). Bottom pressure measurements across the Antarctic circumpolar current and their relation to the wind. *Deep Sea Research A, 27*, 875-888. https://ui.adsabs.harvard.edu/abs/1980DSRA...27..875W